Journal of Materials and Environmental Sciences
ISSN : 2028-2508
CODEN : JMESCN

J. Mater. Environ. Sci., 2020, Volume 11, Issue 2, Page 318-332

http://www.jmaterenvironsci.com

Comparative optimization of removal of low levels of Brilliant Green By ZnOphotocatalysis and photo-Fenton

Yusuf Ibrahim and Umar Ibrahim Gaya

Department of Pure and Industrial Chemistry, Bayero University,700241 Kano P.M.B 3011, Kano State Nigeria.

Received 22 Oct 2019,
Revised 21 Jan 2020,
Accepted 25 Jan 2020

Keywords
- ✓ Photo-Fenton,
- ✓ Brilliant Green,
- ✓ Photo-Catalyst,
- ✓ RSM,
- ✓ Zincoxide.

Ibrahimy864@gmail.com ;
Phone: +2348133376693;
Fax: +2348081352691

Abstract

The degradation of aqueous Brilliant Green (B.G) was investigated using ZnO photo-catalyst and photo-Fenton under visible irradiation. In order to determine the optimum condition the operating parameters of the ZnO Photo-catalyst and photo-Fenton process such as initial dye concentration, initial pH, ZnO dosage, H_2O_2 dosage, and Fe^{2+} dosage have been investigated by the one-factor method and by multivariate analysis. In the multivariate analysis, experimental design based on central composite design (CDD) method was applied to assess the individual and interaction effect of the operating parameters on the degradation efficiency. The kinetics of ZnO photo catalysts Followed pseudo first order kinetics while that of the photo-Fenton process followed pseudo second order kinetics with rate constant of $0.026min^{-1}$ and $0.143min^{-1}$, respectively. Total Organic Carbon (TOC) analysis showed nearly complete mineralization of the dye molecules with slightly higher efficiency for the photo-Fenton process (96%) than the ZnO assisted process (93%).

1. Introduction

Dye industries are important sources of environmental pollution [1 - 2]. After dying, more than 11 % of the dyes are disposed into the environment [3]. Currently, a high number of wastewater treatment technologies are investigated at various levels of operation, and varying degrees of success have been recognized [4 - 5]. Advanced technologies produce hydroxyl radical for exploitation in wastewater treatment. They have the ability to remove pollution and enhance pollutant degradation over the traditional chemical precipitation and adsorption methods. These techniques can be applied successfully to remove contaminant to thus paving way for recycling of the residual water [6]. Special attention has been paid to advanced oxidation processes because of many advantages such as Versatility, safety, selectivity, possibility of automation, environmental friendliness and low investments cost [7 - 8].

Advanced oxidation processes (AOP) involve the production of very reactive oxidants such as $OH^{\cdot}$ (Hydroxyl radical) these processes have the ability to oxidize almost all complex organic pollutant in to two or more smaller molecules or even the complete mineralization of these organic compound in to mainly CO_2, H_2O and inorganic ions [9,10]. Such method of treatments is promising in the remediation of waste waters containing non-biodegradable organic compounds. Hydroxyl radical are extraordinarily reactive and non-selective [11]. The AOP differ from other processes because in AOPs the organic pollutants are degraded rather than concentrated or transferred into a different phase. Moreover, secondary waste materials are not usually generated in the process [12 - 13]. In photo-catalytic degradation of pollutants, TiO_2 has been commonly activated by light to generate the hydroxyl radicals [14 - 15]. Relatively however, ZnO has a great advantage of absorption at a wide fraction of solar spectrum than TiO_2 which makes it a potential substitute especially under visible light irradiation [1,16 - 18]. Fenton was found to be one of the most applied homogeneous AOPs for its ability to degrade high

loading of organic compounds in highly saline conditions [12]. In the process, hydrogen peroxide (H_2O_2) is decomposed by Fe^{2+} in aqueous phase, resulting in the formation of $OH^{\cdot}$. Fenton reagents are widely assisted by irradiation, to realize effective mineralization of contaminants to benign species such as CO_2, water and inorganic salts. The photo-Fenton treatment does not only eliminate toxic substances but increases the biodegradability of the residual water [3].

Brilliant green (BG) dye is used as dye to color fibers, silk, wool, biological stain, veterinary medicine and as an additive to poultry feed to inhibit propagation of mold, intestinal fungus and parasite [19 - 20]. The use of BG dye has been banned in many countries due to its carcinogenic nature [21 - 23]. The demonstration of processes that can remove this compound from aqueous solutions is therefore desirable. In this work we optimized the effectiveness of photo-Fenton and ZnO photo-catalysis for the removal of BG and suggest applicable models for the processes.

2. Material and Methods

2.1 Chemicals:

Brilliant Green Dye (95%) was obtained from Sigma-Aldrich, $FeSO_4.7H_2O$ (99%) was purchased from Sigma, H_2O_2 (40%w/v) from Global Chemie. Other chemicals such as NaOH (99.0%) and H_2SO_4 (96%) from Ideal Scientific, and ZnO (99%) from Analar BDH were used as received, without further purification.

2.2 Experimental procedures:

2.2.1 Photo-Fenton Procedure:

All experimental runs were carried out in a batch reactor containing 100ml solution of BG and ferrous ions. The reaction was initiated by addition of H_2O_2 to the solution. Samples were periodically taken after 1 min interval for first five minute and at 5 min intervals for the remaining 15 min. These samples were immediately analyzed using Perkin-Elmer UV winlab UV-Vis spectrophotometer. Each experiment was repeated three times. The pH of the solution was adjusted to desired level using diluteH_2SO_4 and NaOH.

2.2.2 Photo-catalytic Experiments:

The experiment were carried out in a batch photo reactor containing 100ml dye solution in which ZnO is suspended in desired concentrations. The solutions were continuously magnetically stirred in a dark for at least 30minute to allow equilibrium absorption of the dye molecule on catalyst particles. The pH of was adjusted to the desired level using H_2SO_4 and NaOH. During the reaction experiment 5ml sample of suspension were withdrawn at different time intervals and centrifuge at 3500rpm to remove catalyst particle completely and analyzed using UV-Vis spectrophotometer. Each experiment was repeated three or more times

2.3 Degradation efficiency

The electronic spectrum of brilliant green was recorded over a wavelength ranges 400 800nm using a Perkin Elmer UV winlab UV-Vis spectrophotometer facility. The maximum absorbance wavelength (λ_{max}) of the dye was 624 nm. Therefore, the absorbance of the dye with reaction time was recorded at λ_{max}= 624 nm and concentrations were calculated with aid of calibration curve. In addition, Shimadzu 00077 total organic carbon (TOC) analyzer was used to record depletion of organic carbon. Photo-catalytic degradation/mineralization efficiency of brilliant green was estimated as follows:

$$\text{Performance } \% = \left(1 - \frac{C_t}{C_o}\right) \times 100 \quad \text{..... (1)}$$

C_o is the initial BG concentration or initial TOC BG and C_t is the concentration or TOC of Brilliant green at reaction time t.

2.4 Experimental design

Optimization of parameters of the photo-Fenton and photo-catalysis was carried out using central composite design (CCD) provided by the Design Expert 9.0.6. In the CCD, the total number of experiments (N) is equal to 2^n+2n+6, where n is number of variables. For the photo-catalysis, the independent variables were ZnO dosage, dye concentration, pH and irradiation time, which implies 30 experiments. The design suggests 16 experiments at the cubic points, 8 star or axial experiments and 6 experiments at the centre. There are five input levels (-infinity, low, centre, high, +infinity) of these variable, and five coded (-2, -1, 0, +1, +2) these coded values are displayed in the Table 1.

Table1. Experimental ranges and levels of independent variables for ZnO photo-catalyst.

Independent Variables	Ranges levels				
	-∞ (-2)	Low (-1)	Centre (0)	High(+1)	+∞(+2)
A: Catalyst loading (ZnO g/dm^3)	0.5	1.0	2.0	3.0	3.5
B: Initial dye concentration (mg/dm3)	2.0	3.0	5.0	7.0	8.0
C: Initial solution pH	2.0	3.0	5.0	7.0	8.0
D: Irradiation time (minute)	10	20	50	80	90

For the photo-Fenton process, the independent variables are BG concentration (A), H_2O_2 concentration (B), Fe^{2+} and pH (D) concentration. Accordingly, 30 experiments with five input levels were fitted into the CDD. The coded levels and their corresponding input values are displayed in the Table 2.

Table2. Experimental range and levels of independent variables for Photo-Fenton processes.

Independent Variables	Range Levels				
	-∞ (-2)	Low (-1)	Centre(0)	High(+1)	+∞(+2)
A: BG concentration (mg/dm^3)	4		8	10	12
B: H_2O_2 (mmol/dm^3)	2.6	3.5	4.4	8.8	13.2
C: Fe^{2+} (mmol/dm^3)	0.10	0.15	0.5	0.6	0.65
D: Initial Ph	2	3	4	7	8

3. Results and Discussions:

3.1 Preliminary Studies:

Each of the background process of the photo-Fenton (irradiation, H_2O_2 and Fe^{2+}) has the potential to singly cause the degradation of BG. The effect of these parameters on the degradation of BG is profiled in Figure 1. As seen from the figure, the dark-Fenton (Dark/Fe^{2+}/H_2O_2)gives 57% degradation followed by H_2O_2/UV (44% degradation) and Fe^{2+}/UV (14%).

In the preliminary evaluation of the ZnO-based photo-catalytic degradation of BG however, the concentration of the dye decreased with an increase in reaction time whereas in dark, no significant analytical change was observed.

3.2 Effect of Variable of the ZnO photo-catalysis:

3.2.1 Effect of Catalyst concentration:

To determine the effect of the ZnO loadings, the catalyst concentration was varied from 0.5 to 3.5 g/dm^3. The percentage degradation of BG increased from 0.5 to 2.5 g/dm^3 (Fig.2) followed by decrease to 3.5g/dm^3. The decrease in degradation efficiency, at higher loading levels may be attributed to light scattering by the catalyst particle which attenuates light absorption by the photo-catalyst [24 - 26]. The highest degradation rate (98%) was observed with 2.5g/dm^3 of the catalyst, which corresponds to the optimum concentration.

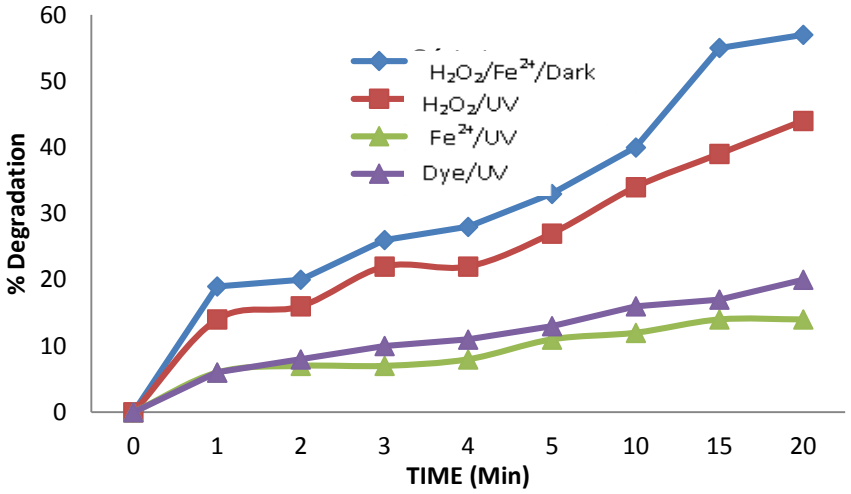

Fig.1. Degradation profile of BG in different systems: H_2O_2/Fe^{2+}/Dark, H_2O_2/UV, Fe^{2+}/UV, and Dye/UV against time.

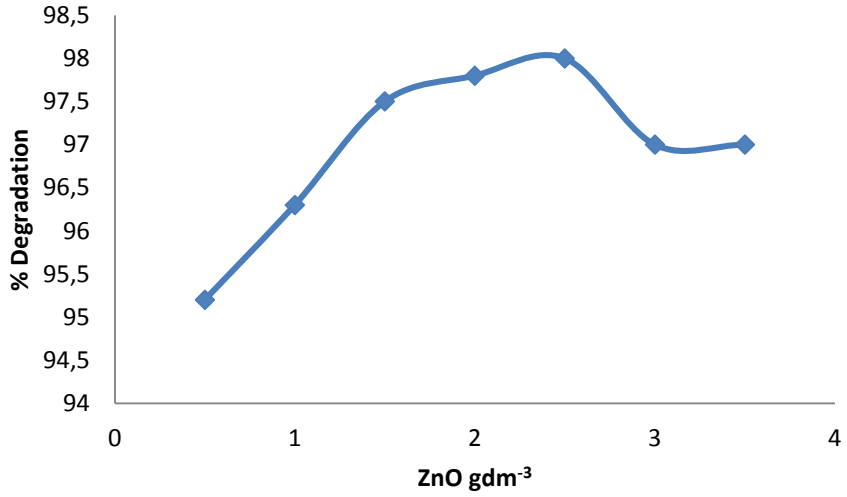

Fig.2: Percentage degradation of BG at varying concentration of ZnO pH = 7 and BG concentration 4 mg/dm^3 at wavelength 624 nm.

3.2.2 Effect of BG Concentration:

The effect of BG concentration was investigated by varying the initial concentration from 2 to 8mg/dm^3 and result are shown in figure 3. As seen from the figure, the degradation is was optimum (98%) at initial dye concentration from 2mg/dm^3. An increase in the initial BG concentration up to 8mg/dm^3 shows increase in the inhibition efficiency, likely due to lower photonic absorption of the catalyst system. The increase in dye concentration obstructs the penetration of photons entering into the solution, leading to less production of hydroxyl radicals [5, 27 - 28].

3.2.3 Effect of pH for ZnO-assisted process:

The pH effect on the degradation of BG studied in the pH range limited to 2-9 as shown in figure 4, by considering the solubility of ZnO in acidic as well as highly basic solutions. The percentage degradation of the dyes shows increase with increase in pH from 2 to 7 and then decrease with increase of pH from 7 to 9. The most favorable degradation was achieved at pH of 7. These observations may be linked to the amphoteric nature of ZnO at highly acidic pH can react to produce corresponding salt while at highly alkaline pH it can react with base to form complex like $[Zn(OH)_4]^{2-}$ [1, 29]. Hence pH 7 was utilized in further studies.

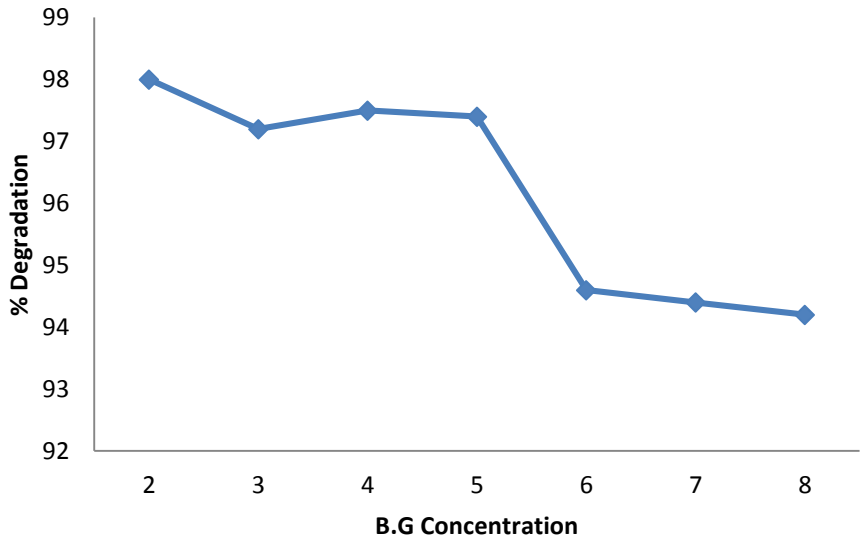

Fig.3. Percentage degradation of BG at varying concentrations of BG, ZnO=2.5g/dm^3 and pH=7.

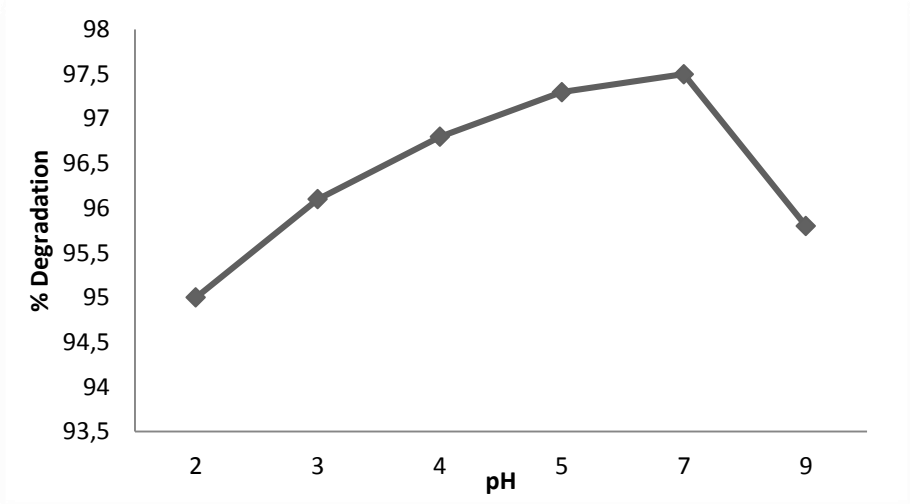

Fig.4. Percentage degradation of BG at varying pH, [BG] =4mg/dm3,andZnO = 2.5 g/L.

3.3 Effect of Variables of the photo-Fenton Processes

3.3.1 Effect of H_2O_2 Dosages:

The effect of addition of H_2O_2 (2.6 to 13.2 mmol/dm^3) on the degradation of BG is shown in Fig.5 From the figure, the addition of 4.4mmol/dm^3 H_2O_2 had the highest effect (98%) on the degradation of BG by photo-Fenton process. A higher amount of hydrogen peroxide causes no significant change in degradation due to the competing scavenging reaction of hydroxyl radicals with the H_2O_2 [12, 22] as expressed below:

$$OH^{\cdot} + H_2O_2 \longrightarrow H_2O + HO_2^{\cdot} \qquad (2)$$

$$HO_2^{\cdot} + OH^{\cdot} \longrightarrow H_2O + O_2 \qquad (3)$$

3.3.2 Effect of Fe^{2+} Dosage:

The amount of ferrous is one of the main parameters that influenced photo-Fenton process. The effect of addition of fe^{2+} was studied in the range of 0.15 to 0.65mmol/dm^3 (Fig.6). Generally speaking, iron acts as catalyst and not participate in the reaction but enhance the oxidation process. In this study, the maximum degradation (98%) was achieved at 0.15 mmol/dm^3 iron dosage. Hence, 0.15mmol/dm^3 was

considered as the optimum dosage of iron for the study. In excess Fe^{2+}, a great amount of Fe3+ from the process of H_2O_2 decomposed by Fe^{2+} was easy to exit in the form of $Fe(OH)^{2+}$ in acidic environment which would compete for light absorption thus decreasing the extant of degradation [30].

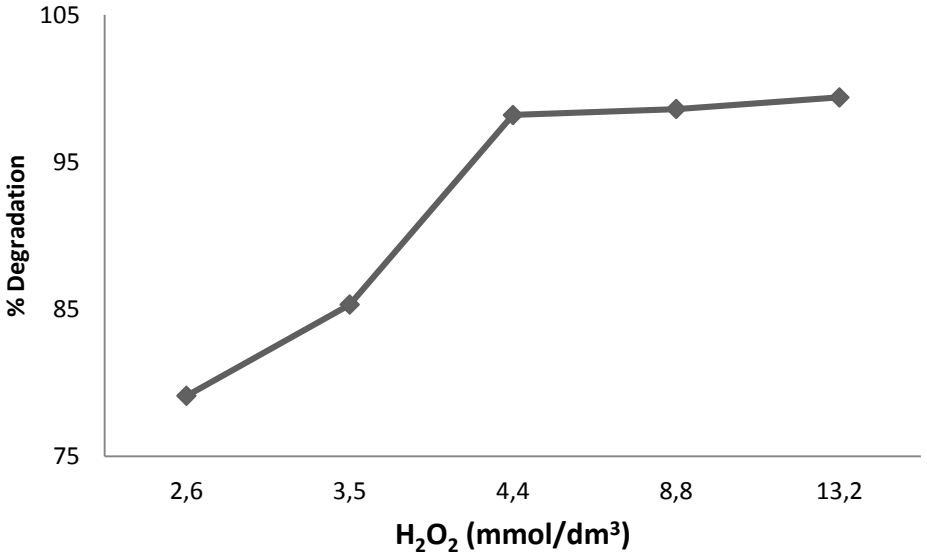

Fig.5. Degradation of BG as function of H_2O_2 concentration. Reaction conditions: Fe^{2+}= 0.15 mmol/dm^3pH of 3, dye concentration of 8mg/dm^3, at 624nm wavelength the reaction completed in 20 min.

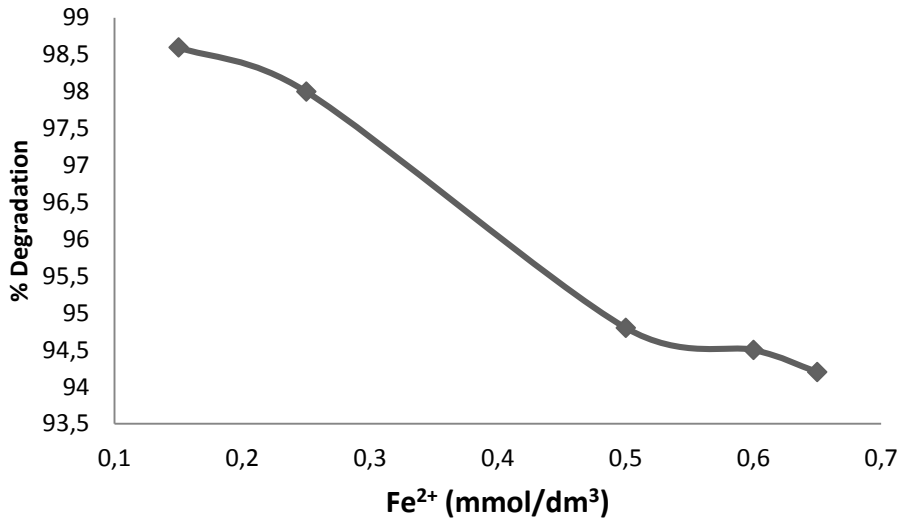

Fig.6. Degradation efficiency of BG at varying concentrations of Fe^{+2} [H_2O_2] =4.4mmol/dm^3 and pH=3.

3.3.3 Effect of BG for photo-Fenton process

The B.G concentration is one of the important parameters in photo-Fenton processes. The effect of initial dye concentration in these processes is shown in Fig.7. The figure clearly reveals increase in the highest degradation efficiency at 8 mg/dm^3 initial dye concentration. Above this dose the degradation efficiency decreases steadily, most likely due to poor absorption of light photons [2, 27 - 28].

3.3.4 Effect of pH for photo-Fenton process

The effect of pH on the degradation of BG by photo-Fenton process is shown in Fig.8. The photo-Fenton process was most favorable at pH 2, and could be inhibited by increasing pH from 3 to 7 (Fig. 8). The decrease in degradation efficiency may be as a result of low production of hydroxyl radicals from the irradiated Fenton system [30 -32].

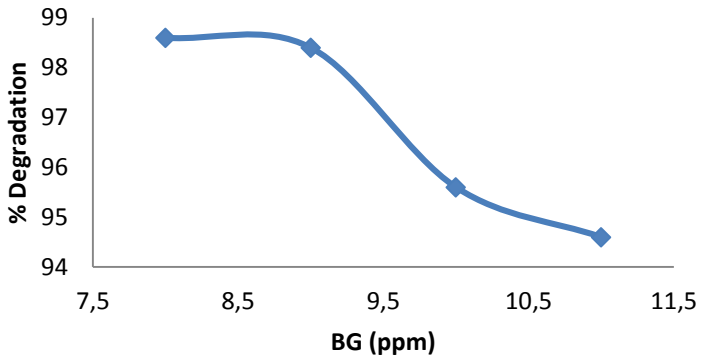

Fig.7. Degradation efficiency of BG as function of dye concentration, Reaction conditions: pH = 3, H_2O_2 dosage = 4.4mmol/dm^3 and Fe^{2+} dosage = 0.15mmol/dm^3.

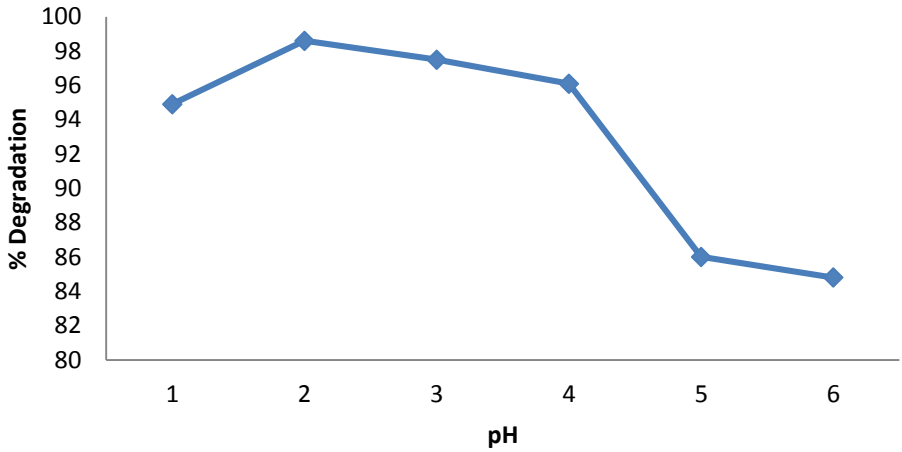

Fig.8. Degradation of BG as function of pH. [Fe^{+2}] = 0.15mmol/dm^3 and [H_2O_2] = 4.4 mmol/dm^3.

3.4 Mineralization of BG:

In order to assess the degree of mineralization during the photo-Fenton and the ZnO-assisted process, total organic carbon (TOC) was monitored. The mineralization of BG for the ZnO photo-catalysis reached 93%, achieved after 90min of irradiation time while for photo-Fenton process the mineralization efficiency was 96% (achieved within 20 min of irradiation time).

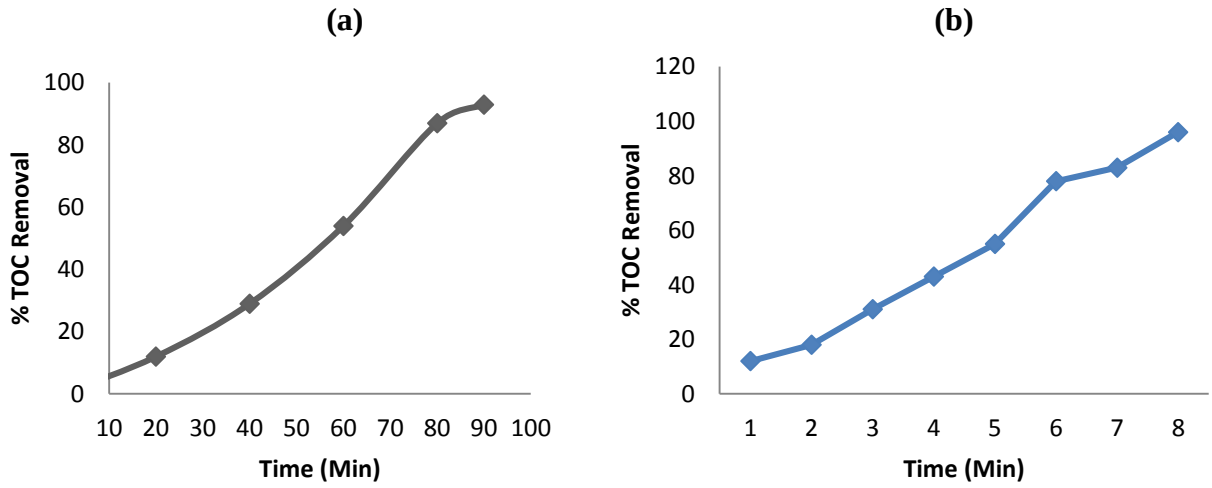

Fig.9.(a) Plot % TOC removal against Time (min) for ZnO photo-catalyst. (b) Plot % TOC removal against time (min) for photo-Fenton process

3.5 Kinetic Studies:

The kinetics of the degradation of BG was tested using pseudo first order and pseudo second order integrated rate laws expressed by equations (4) and (5).

$$\ln C_t = -k_1 t + \ln C_0 \qquad (4)$$

$$\frac{1}{C_t} = k_2 t + \frac{1}{C_0} \qquad (5)$$

Where C_t is the concentration of BG at time t and C_o is the initial concentration.

The kinetic parameters for both the photo-Fenton and the ZnO photo-catalytic processes are shown in Table 3. Based on the coefficients of determination (R^2), the ZnO-photo-catalysis follows pseudo first order kinetics with the rate constant (k) value of $0.026 min^{-1}$. On the other hand, the photo-Fenton process agrees with pseudo second order kinetics with rate constant value of $0.9580 Lmol^{-1}min^{-1}$.

Table.3: Summary of Kinetic Studies for Fenton-ZnO Photo-catalysis.

Photo-catalyst	Pseudo First Order		Pseudo Second Order	
	k	R^2	k	R^2
ZnO	0.026	0.948	0.143	0.816
Fenton	0.063	0.882	0.958	0.971

3.6 Band Gap Energy (E_g) of ZnO

Determining the band gap of ZnO is important to know the wavelength by which the semiconductor photocatalyst can be excited. The band gap (E_g) of ZnO was estimated using Kubelka-Munk equation (6) [18].

$$Kh\nu = C_i[h\nu - E_g]^{1/2} \qquad \ldots\ldots\ldots\ldots\ldots (6)$$

Where K is absorption function (recorded on UV-Vis spectrometer).

The intercept of the plot of natural log of remission function (lnK) against photon energy (*hv*) (Fig.10) provided the band gap value of 3.37*ev*.

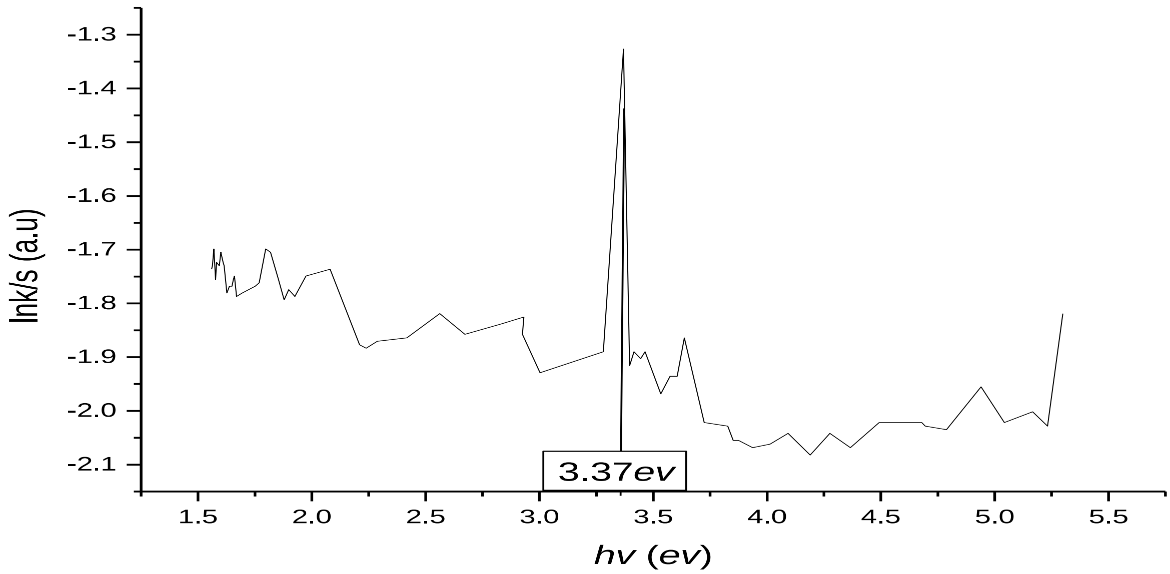

Fig.10. Plot of lnk against photon energy (hv) for ZnO catalyst.

3.7 Multivariate analysis

The 4-factor CDD matrix of the photo-Fenton process, its experimental and predicted results obtained are presented in Table 4. All variables can be correlated by a second order polynomial response equation (7). The results in table 4 show good agreement between the experimental and predicted values of degradation efficiency.

Experimental efficiency % for photo-Fenton process = $77.50 - 11.83A + 2.92\mathbf{B} - 9.00C + 4.08D - 3.63AB + 1.88AC + 1.75\ AD + 5.63BC - 1.50BD - 1.00CD - 0.083A^2 + 0.79B^2 - 13.58C^2 - 0.083D^2$ …….. (7)

Where A = Fe^{2+} Dosage B= H_2O_2, C=initial pH and D=BG concentration.

Table.4: Input domains and corresponding experimental and predicted values of photo-Fenton efficiency.

Run	Fe^{2+} ($mmol/dm^3$)	H_2O_2 ($mmol/dm^3$)	pH ($mmol/dm^3$)	B.G (mg/dm3)	Experimental %	Predicted %
1	1	-1	1	-1	31	21
2	0	0	0	0	75	79
3	0	0	-2	0	33	31
4	0	0	2	0	7	12
5	1	-1	-1	1	80	79
6	2	0	0	0	49	47
7	1	1	-1	-1	45	49
8	0	0	0	0	81	79
9	-1	-1	1	1	57	55
10	0	0	0	0	76	79
11	1	-1	1	1	46	44
12	1	1	1	-1	53	51
13	-1	1	-1	-1	96	95
14	-1	-1	-1	-1	78	82
15	0	-2	0	0	69	71
16	-1	-1	-1	1	94	91
17	0	0	0	0	75	79
18	0	0	0	0	75	79
19	-1	-1	1	-1	58	56
20	0	0	0	-2	65	62
21	1	1	1	1	55	53
22	0	2	0	0	86	89
23	0	0	0	2	83	85
24	-1	1	1	1	77	73
25	-1	1	-1	1	91	93
26	0	0	0	0	83	79
27	-1	1	1	-1	70	69
28	-2	0	0	0	99	98
29	1	-1	-1	-1	67	66
30	1	1	-1	1	60	58

The variables in the CCD matrix of the ZnO photo-catalysis as well as its experimental and predicted results are presented in Table 5. The results also fitted a second order polynomial model (equation (12)). The result indicated good agreements between the experimental and predicted values of the dye removal efficiency:

Exp (%) = +57.560 + 1.437A - 2.667B +5.764C +25.756D +0.919AB - 0.198AC - 2.859AD - 0.971BC + 4.173BD + 0.843CD + 1.903A^2 + 1.282B^2 - 4.591C^2 - 0.774D^2 …….. (8)

Where A = Catalyst Loading (g/l), B = initial dye concentration (mg/dm^3), C = pH of the solution and D = Irradiation time (min).

Table.5: Experimental and predicted value of ZnO-assisted photodegradation efficiency.

Run	Catalyst loading	Initial dye concentration	Initial solution pH	Irradiation Time	Experimental %	Predicted %
1	1	1	1	-1	28.56	28.56
2	-1	1	-1	-1	21.3	18.3
3	0	0	0	0	55.4	68.4
4	0	0	0	2	99	99
5	-1	1	1	-1	24.38	24.38
6	-2	0	0	0	57.5	57.5
7	0	0	0	0	67.61	67.61
8	1	-1	-1	1	67.21	67.21
9	0	-2	0	0	70.78	70.78
10	-1	-1	-1	1	78.26	78.26
11	-1	-1	-1	-1	16.54	16
12	1	1	1	1	98	99
13	1	-1	1	-1	47.55	47.55
14	1	-1	1	1	77.66	77.66
15	0	2	0	0	53.76	55.76
16	0	0	0	-2	9.09	9.09
17	-1	-1	1	-1	37.75	37.75
18	0	0	2	0	44.52	46
19	2	0	0	0	72.01	72.01
20	-1	-1	1	1	99.61	99.61
21	1	-1	-1	-1	35.12	35.12
22	0	0	0	0	55.46	59.46
23	0	0	0	0	55.62	46.62
24	0	0	-2	0	33.03	33.03
25	0	0	0	0	55.74	57.74
26	1	1	-1	1	79	79
27	-1	1	-1	1	75.26	75.26
28	-1	1	1	1	88.88	88.88
29	1	1	-1	-1	14.35	14.35
30	0	0	0	0	55.53	53.53

The results of analysis of variance for the photo-Fenton model are shown in table 6 while those of ZnO photo-catalysis are displayed in Table 7. Statistically, the correlation co-efficiency (R^2) quantitatively evaluates the correlation between the experimental data and the predicted responses. The predicted values of both models matched the experimental values reasonably well with R-square values of 0.9561 and 0.9522 (which are close to 1) for the photo-Fenton and ZnO photo-catalysis, respectively. This implies that about 96% of changes in the data can be explained by the model the variation for percentage degradation are explained by the independent variables and this also means that the model does not explain only about 3.8% of variation. Adjusted R^2 (Adj-R^2) is also measure of goodness of a fit, but it is more suitable for comparing models with different numbers of independent variables. The predicted R^2 are in reasonable agreement with adjusted R^2 (see Table 6 and 7) therefore the different is less than 0.2, the model has an adequate precision greater than 4.00 which shows that it is desirable and implies an adequate signal. This also indicates that the model can be used to navigate the design space.

Table.6: ANOVA for response Surface Quadratic Model Analysis of Variance for ZnO.

Factors	Degree of freedom	Standard error	F-Value	P-Value Prob>F	
Model	14		21.33	<0.0001	Significant
Intercept	1	3.19			
A-ZnO	1	1.60	0.81	0.3819	
B-B.G	1	1.60	2.80	0.1153	
C-pH	1	1.60	13.05	0.0026	
D-Time	1	1.60	260.67	< 0.0001	
AB	1	1.95	0.22	0.6447	
AC	1	1.95	0.010	0.9206	
AD	1	1.95	2.14	0.1640	
BC	1	1.95	0.25	0.6265	
BD	1	1.95	4.56	0.0496	
CD	1	1.95	0.19	0.6722	
A^2	1	1.49	1.63	0.2215	
B^2	1	1.49	0.74	0.4037	
C^2	1	1.49	9.47	0.0077	
D^2	1	1.49	0.27	0.6115	
Lack of fit	10		3.28	0.1011	Not significant
		Stddev	7.82	R-square	0.9522
		Mean	55.82	Adj. R-square	0.9075
		CV%	14.00	Pred.R-square	0.7518
		PRESS	4753.19	Adeq. Precision	18.643

Table.7: ANOVA for Response Surface quadratic Model Analysis of Variance for Fenton process

Factors	Degree of freedom	Standard error	F-value	P-Value Prob>F	
Model	14		21.05	<0.0001	Significant
Intercept	1	2.62			
A- Fe^{2+}	1	1.31	81.39	<0.00001	
B-H_2O_2	1	1.31	4.94	0.0420	
C- pH	1	1.31	47.08	<0.0001	
D-B.G	1	1.31	9.69	0.0071	
AB	1	1.61	5.09	0.0394	
AC	1	1.61	1.36	0.2614	
AD	1	1.61	1.19	0.2932	
BC	1	1.61	12.26	0.0032	
BD	1	1.61	0.87	0.3652	
CD	1	1.61	0.39	0.0430	
A^2	1	1.23	4.613E003	0.3467	
B^2	1	1.23	0.42	0.0285	
C^2	1	1.23	122.57	< 0.0001	
D^2	1	1.23	4.613E003	0.9467	
Lack of fit	10		4.38	0.0585	Not significant
		Stddev	6.43	R-square	0.9516
		Mean	67.13	Adj. R-square	0.9064
		CV%	9.57	Pred.R-square	0.7425
		PRESS	3293.04	Adeq. Precision	21.055

The lack of fit values of 0.0585 and 0.1011 for the photo-Fenton and ZnO photo catalysis respectively, indicate that the lack of fit is not significant relative to pure error [33]. Insignificant lack of fit is good for the model. The P-value was used as a tool to check the significance of each of the coefficients, which in turn, are necessary to understand the pattern of the mutual interaction between the test variables. The smaller the P-values, the bigger the significant of the corresponding coefficients, the more significant is the corresponding coefficients. The ANOVA of the model F=4.381, p<0.0001 and 21.33, p<0.0001 for both process respectively are significant there is only 0.01% chance that an F-value this larger could occur due to noise [22, 34].

3.7.1 Response surface

Interpretation about photo systems with multiple input variables and output is greatly enhanced by the use of surface diagrams. In Fig. 11(a), the response was plotted as a function of initial dye concentration and pH while the initial Fe^{2+} concentration and H_2O_2 were kept constant (0.5 mmol/dm^3 and 4.4 mmol/dm^3) being the central levels. As seen in Fig.11(a) the degradation increase with increase in pH and decrease with increase in pH, the extent of the increase start from minus infinity to the centre and then decrease from centre to plus infinity. This behavior is one of the characteristic of advanced oxidation process (AOP). On the other hand, Fig. 11(b) shows the response surface plot of the degradation efficiency as function of H_2O_2 and initial pH. From the figure, the degradation efficiency increase with increase in H_2O_2, This may be due to the greater production of $\cdot OH$, the maximum production of $\cdot OH$ via Fenton's reaction take place at the optimized H_2O_2 contents.

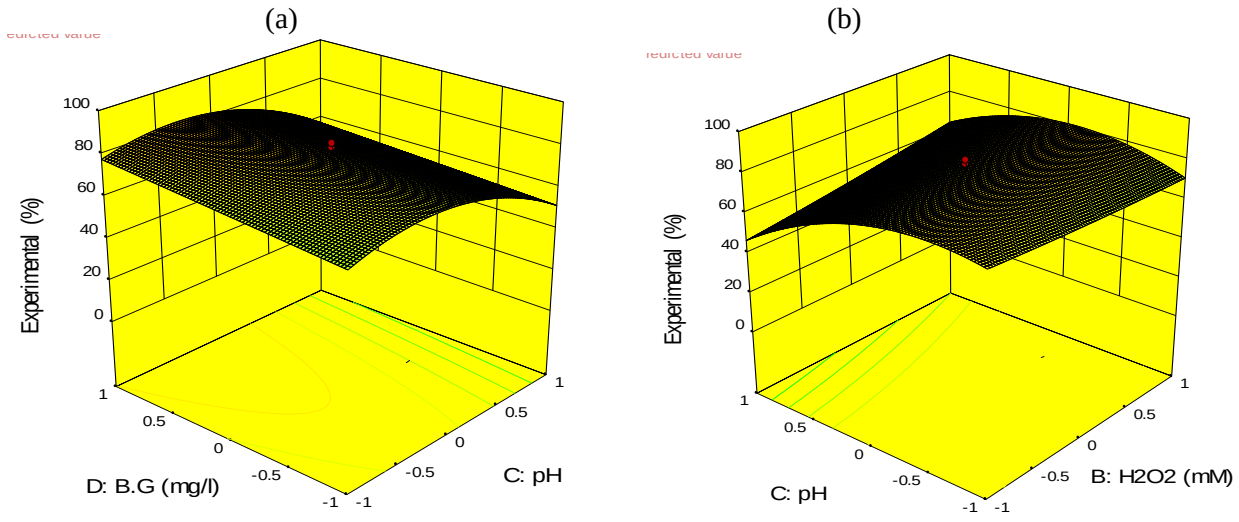

Fig.11. (a)Three dimensional response surface plot of percentage degradation as a function of ph and BG concentration. (b) Three dimensional response surface plots of percentage degradation as a function of pH and H_2O_2 dosage for Photo-Fenton process respectively.

The response surface plots of photo-catalytic degradation efficiency as a function of ZnO concentration and BG concentration (at fixed pH of 5 and reaction time 50min) is displayed by Fig. 12(a). As in the figure, increase in ZnO concentration increases the degradation efficiency of the dye while the increase of BG concentration shows the decrease in degradation efficiency. Similarly, Fig. 12(b) shows the response surface plots of the degradation efficiency as function of irradiation time and initial pH. The degradation efficiency increase with time which shows that time is the key factor in the degradation of

BG [35]. As in fig. 12(b), the degradation of BG show an increase proportionally with increase in pH and then decrease of the removal efficiency at higher pH values.

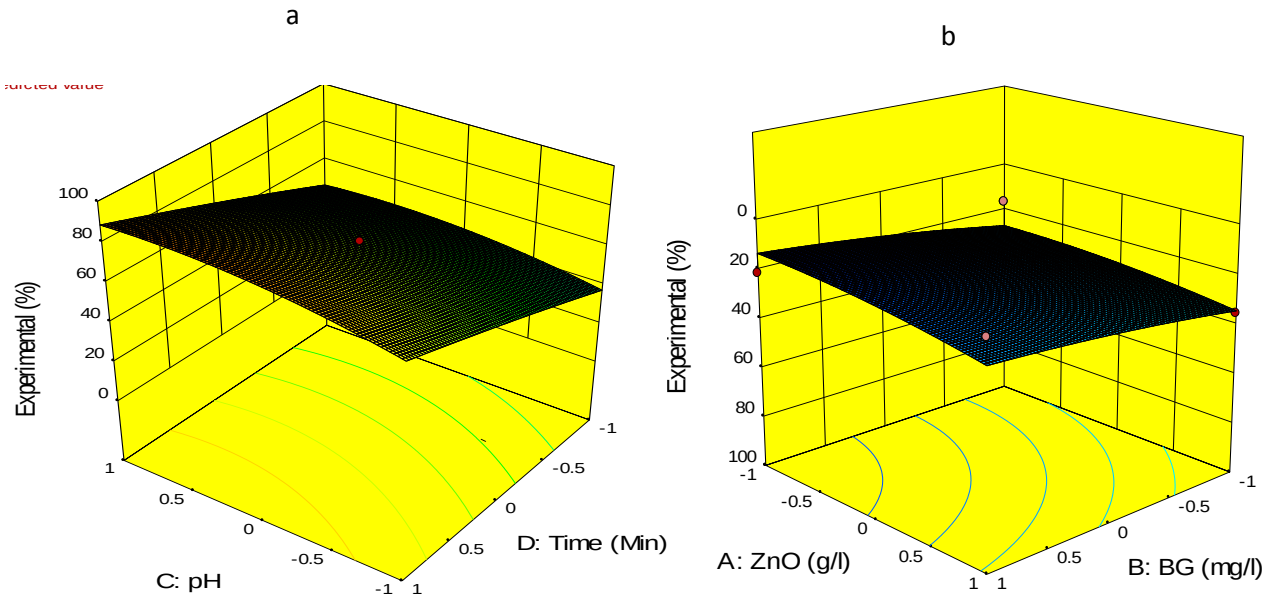

Fig.12. (a) three dimensional response surface plots of percentage degradation as a function of pH and time. (b) Three dimensional response plot of percentage degradation as a function of ZnO concentration and BG concentration for ZnO Photo-catalytic process

Conclusion

In this study the removal of brilliant green dye by photo-Fenton and ZnO photo-catalysis has been optimized. For photo-Fenton process the optimum conditions of operating variables were 4.4 mmol/dm^3 H_2O_2, 0.15m mol/dm^3 Fe^{2+} and 8mg/dm^3 Brilliant green. Under these conditions, 99% degradation and 96% mineralization were achieved in 20 min irradiation time. For ZnO photo-catalysis, the optimum conditions were ZnO 2.5g/l, solution pH 7 and 4mg/l dye concentration. Degradation and mineralization efficiencies of 98% and 93% respectively were achieved within 90 min of irradiation. For the photo-Fenton, degradation follows pseudo second order while the ZnO-mediated photo-catalytic process follows pseudo first order. Factorial experimental design based on central composite design was successfully used to model these degradation profiles.

References

1. V. Pare, S.B. Jonnalagadda, H. Tomer, P. Singh, V.W. Bhagwat, ZnO assisted Photocatalytic degradation of Acridine Orange in Aqueous solution using visible irradiation, *Desalination* 232 (2008) 80-90.
2. RahatJavaid, and UmairYaqubQaziCatalytic Oxidation Process for the Degradation of Synthetic Dyes: An Overview, *International Journal of Environmental Research and Public Health* 16 (2019)11: 2066.
3. J.H. Sun, S.P. Sun, G.L Wang, and L.P. Qiao, Degradation of azo dye Amido black 10B in Aqueous Solution by Fenton Oxidation Process. *Journal of Dyes and Pigments* 7 (2007) 647-652.
4. S.Z. Chen, P.Y. Zhang, W.P. Zhu, L. Chen, S.M. Xu, Deactivation of TiO_2photocatalytic films loaded on aluminum: XPS and AFM analyses, *Appl. Surf. Sci*. 252 (2006) 7532-7538.
5. Shiljashree Vijay, Raj Mohan Balakrishnan, Eldon R. Rene and Uddandarao Priyanka, Photocatalytic degradation of Irgalite violet dye using nickel ferrite nanoparticles *Journal of Water Supply: Research and Technology - AQUA*68 8 (2019) 666 - 674
6. H. Zhou, and D.W. Smith. Advanced technologies in water and wastewater treatments. *Journals of Environmental Engineering Sciences* 1 (2002) 247–264.
7. C.C. Chen, C.S. Lu, H.J. Fan, W.H. Chung, J.L. Jan, H.D. Lin, W.Y. Lin, Photocatalyzed *N*-deethylation and degradation of Brilliant Green in TiO_2 dispersions under UV irradiation, *Desalination* 219 (2008) 89 – 100.

8. H.K. Hansen, P. Nunez, D. Raboy, I. Schippacasse, R. Grandon. Electro coagulation in wastewater containing arsenic: Comparing different process designs, *Electrochimica Acta*, 52 (2007) 3464-3470.
9. N. Klamerth, L. Rizzo, S. Malato, M.I. Maldonado, A. Aguera, and A.R. Fernandez-Alba. Degradation of Fifteen Emerging Contaminants at µg L^{-1} Initial Concentrations by mild solar photo-Fenton in MWTP effluents. *Water Research*. 44 (2010)545 - 554.
10. J.-B. Tarkwa, N. Oturan, E. Acayanka, S. Laminsi, M.A. Oturan, Photo‑Fenton oxidation of Orange G azo dye: process optimization and mineralization mechanism, *Environmental Chemistry Letters*, 17 (2019) 473–479.
11. M. Klavarioti, D. Mantzavinos, D. Kassinos. Removal of residual pharmaceuticals from aqueous systems by advanced oxidation processes. *Environ. Int.* 35 (2009) 402 – 417.
12. K. Amerpret, *Degradation and decolourisation of Reactive Black Dye using SonoPhoto Fenton*, (Unpublished master's thesis). Thapar University Patiala, Punjab (2012).
13. Sennaoui A., S. Alahiane, F. Sakr, A. Assabbane, El H. Ait Addi, M. Hamdani, Advanced Oxidation of Reactive Yellow 17 Dye: a Comparison between Fenton, Photo-Fenton, Electro-Fenton, Anodic Oxidation and Heterogeneous Photocatalysis Processes. *Portugaliae Electrochimica Acta* 36 (2018)163-178.
14. W. Baran, A. Makowski, W. Wardas, The effect of UV radiation absorption of cationic and anionic dye solutions on their photocatalytic degradation in the presence TiO_2, *Dyes and Pigments* 76 (2008) 226 – 230.
15. M.A. Lazar, S. Varghese, and S.S. Nair, Photocatalytic Water Treatment by Titanium Dioxide: Recent Updates, *Catalysts*. 2 (2012) 572 – 601.
16. Bhaviya Raj R., Uma devi M. Parimaladevi R., Enhanced photocatalytic degradation of textile dyeing wastewater under UV and visible light using ZnO/MgO nanocomposites as a novel photocatalyst, *Particulate Science and Technology*, DOI:10.1080/02726351.2019.1616863
17. Xiaoqing Chen, Zhansheng Wu, Dandan Liu and Zhenzhen Gao, Preparation of ZnO Photocatalyst for the Efficient and Rapid Photocatalytic Degradation of Azo Dyes. *Nanoscale Research Letters* 12 (2017) 143
18. U.I. Gaya, Comparative Analysis of ZnO Catalyzed Photo-Oxidation of P Chlorophenols. *European Journal of Chemistry* 2 (2011) 163-167.
19. Y.D. Thakare and M.S. Jadav. Degradation of Brilliant Green dye using Cavitations based Hybrid Techniques *International Journal of Advance Engineering Technology* (2013) 31-36.
20. Murilo Gonçalves da Rocha, Shirley Nakagakia, Geani Maria Ucoskia, Fernando Wypycha, GuilhermeSippelMachadob. Comparison between catalytic activities of two zinc layered hydroxide salts in brilliant green organic dye bleaching, *Journal of Colloid and Interface Science* 541 (2019) 425–433
21. P.R. Gogate and G.S. Bhosale. Comparison of Effectiveness of Caustic Cavitations and Hydrodynamic Cavitation in Combined Treatment Scheme for Degradation of Dye Waste Waters. *Chem. Eng. Proc: Process Intensification* 71 (2013) 59 – 69.
22. PankajTaneja, Shelja Sharma, Ahmad Umar, Surinder Kumar Mehta, Alex O. Ibhadon, Sushil Kumar KansalVisible-light driven photocatalytic degradation of brilliant green dye based on cobalt tungstate ($CoWO_4$) nanoparticles :*Materials Chemistry and Physics* S0254-0584(2018)30145-7
23. Shawky M. Hassan A, Mohammed A. Mannaa B, Photocatalytic Degradation of Brilliant Green Dye by SnO_2/TiO_2Nanocatalysts*International Journal of Nano and Material Sciences*, 5(1) (2016) 9-19
24. A. Akyol, M. Bayramoglu. Photocatalytic degradation of Remazol Red F3B using ZnO Catalyst *Journal of Hazardous Materials* 124 (2005) 241-246.
25. Chijioke-Okere O. Maureen, Okorocha J. Nnaemeka, Anukam N. Basil1, Oguzie E. Emeka, Photocatalytic Degradation of a Basic Dye Using Zinc Oxide Nanocatalyst, *International Letters of Chemistry, Physics and Astronomy* (81) (2018) 18-26.
26. Saeid Taghavi Fardood, Ali Ramazani, Sajjad Moradi, Pegah Azimzadeh Asiabi, Green synthesis of zinc oxide nanoparticles using arabic gum and photocatalytic degradation of direct blue 129 dye under visible light *Journal of Material Science: Material in Electronics* 28 (2017) 18: 13596 – 13601.
27. J. Feng, X. Hu, P.L. Yue, H.Y. Zhu, Q.G. Lu, Decolourisation and Mineralization of reactive red HE-3D by Heterogeneous Photo Fenton reaction. *Water Research*, 37 (2003) 3776 -3784.
28. J. Gallo, J. Borja, S. Gallardo,, C. Salim, P. Ngaotrakanwiwat, H. Hinodo. Optimization for Photocatalytic Color Removal of Turquoise Blue Dye C.I 199 In Immoblized Ac/TiO_2 and UV-System using Response Surface Methodology, *Tokyo Instate of Technology*, 64 (2012) 73.

29. Dilaeleyana Abu Bakar Sidik, Nur Hanis Hayati Hairom, Nur Zarifah Zainuri, Amira Liyana Desa, Nurasyikin Misdan, Norhaniza Yusof, Chin Boon Ong, Abdul Wahab Mohammad, Nur Shahirah Mohd Aripen, Photocatalytic Degradation Of Industrial Dye Wastewater Using Zinc Oxide-Polyvinylpyrrolidone Nanoparticles *Malaysian Journal of Analytical Sciences*, 22 (2018) 693 - 701
30. X.k. Zhao, G.P. yang, Y.J. Wang, X.C. Gao Photochemical degradation of dimethyle phthalate by Fenton reagent, *Photochemistry and photo biology A: Chemistry* 161 (2004) 215 - 220.
31. G.W.T Spins, R. Woods. *Introduction to radiation* chemistry Book New York: John Wiley and sons 3rd edition, (1990) P. 130.
32. Mohammed Shaban, Mostafa R. Abukhadra, Suzan S. Ibrahim, Mohammed G. Shahien, Photocatalytic and photo-Fenton oxidation of Congo Red dye Pollutants in Water Using Natural Chromite – Response Surface Optimization. *Applied Water Science* 07 (2017) 4743 – 4756.
33. Xiangfeng and Yalei Zhao. Optimization of photocatalytic degradation of dye wastewater by $CuFe_2O_4$/AgBr composite using response surface methodology. *Material Research. Express* 06 (2018) 3:036109.
34. Rania Farouq, M. Abd-Elfatah and M. E. Ossman. Response surface methodology for optimization of photocatalytic degradation of aqueous ammonia *Journal of Water Supply: Research and Technology—AQUA* (2018) 121.
35. Nahid Khoshnamvand, Ferdos Kord Mostafapour, Amir Mohammadi and Maryam Faraji, Response surface methodology (RSM) modeling to improve removal of ciprofloxacin from aqueous solutions in photocatalytic process using copper oxide nanoparticles (CuO/ UV) *AMB Expr* 8 (2018) 48

(2020) ; http://www.jmaterenvironsci.com